

AD-A113 671

HARRY DIAMOND LABS ADELPHI MD
ANALYSIS OF THE ELECTROMAGNETIC MODES PROPAGATED ON AN ELECTRON--ETC(U)
APR 82 G D DOCKERY, C A MORRISON
HDL-TR-1982

F/G 20/8

UNCLASSIFIED

NL

1 of 1
AD A
113 671

END
DATE
FILED
05-82
DTIC

AD A113671

UNCLASSIFIED

SECURITY CLASSIFICATION OF THIS PAGE (When Data Entered)

REPORT DOCUMENTATION PAGE		READ INSTRUCTIONS BEFORE COMPLETING FORM
1. REPORT NUMBER HDL-TR-1982	2. GOVT ACCESSION NO. AD 423571	3. RECIPIENT'S CATALOG NUMBER
4. TITLE (and Subtitle) Analysis of the Electromagnetic Modes Propagated on an Electron Beam		5. TYPE OF REPORT & PERIOD COVERED Technical Report
		6. PERFORMING ORG. REPORT NUMBER
7. AUTHOR(s) G. Daniel Dockery Clyde A. Morrison		8. CONTRACT OR GRANT NUMBER(s)
9. PERFORMING ORGANIZATION NAME AND ADDRESS Harry Diamond Laboratories 2800 Powder Mill Road Adelphi, MD 20783		10. PROGRAM ELEMENT, PROJECT, TASK AREA & WORK UNIT NUMBERS Program Ele: 6.11.01.A
11. CONTROLLING OFFICE NAME AND ADDRESS U.S. Army Materiel Development and Readiness Command Alexandria, VA 22333		12. REPORT DATE April 1982
		13. NUMBER OF PAGES 44
14. MONITORING AGENCY NAME & ADDRESS (if different from Controlling Office)		15. SECURITY CLASS. (of this report) UNCLASSIFIED
		15a. DECLASSIFICATION/DOWNGRADING SCHEDULE
16. DISTRIBUTION STATEMENT (of this Report) Approved for public release; distribution unlimited.		
17. DISTRIBUTION STATEMENT (of the abstract entered in Block 20, if different from Report)		
18. SUPPLEMENTARY NOTES DRCMS Code: 61110191A0011 DA Project: 1L161101A91A HDL Project: A10036		
19. KEY WORDS (Continue on reverse side if necessary and identify by block number) E-beam modes Electron beams Millimeter waves Slow waves		
20. ABSTRACT (Continue on reverse side if necessary and identify by block number) The relationship of electron density, n , current density, J , and electric field, E , for an electron beam is derived by using Maxwell's equations and the Lorentz force equation. The resulting wave equations are solved for a ribbon electron beam and a cylindrical beam. It is shown that there exist modes propagating along the beam much the same as waves in dielectric waveguides. However, unlike dielectric waveguides, the number of		

Part A →

UNCLASSIFIED

SECURITY CLASSIFICATION OF THIS PAGE(When Data Entered)

modes of an electron beam is doubly infinite. One set of waves propagates along the beam with phase velocity greater than the speed of the electrons in the beam. The other set has the phase velocity less than the electrons. The phase velocity of both sets of waves approaches the electron velocity for very large mode number. The total energy propagated down the electron beam is given, and the fraction of energy outside the beam is shown to be larger for a cylindrical beam than for a ribbon beam.

Accession For	
NTIS GRA&I	<input checked="" type="checkbox"/>
DTIC TAB	<input type="checkbox"/>
Unannounced	<input type="checkbox"/>
Justification	
By _____	
Distribution/ _____	
Availability Codes	
Dist	Avail and/or Special
A	



A

UNCLASSIFIED

2 SECURITY CLASSIFICATION OF THIS PAGE(When Data Entered)

CONTENTS

	<u>Page</u>
1. INTRODUCTION	5
2. ELECTRON BEAM WAVE EQUATIONS	6
3. RESTRICTED BEAM	10
3.1 Ribbon Beam	12
3.2 Cylindrical Beam	16
4. ANALYSIS OF BEAMS	19
4.1 Analysis of Ribbon Beam	19
4.2 Analysis of Cylindrical Beam	29
5. CONCLUSIONS	39
ACKNOWLEDGEMENT	40
LITERATURE CITED	41
DISTRIBUTION	43

FIGURES

1 Behavior of $Z \tan Z$ as function of Z demonstrating periodicity of values of Z that satisfy equation (73)	23
2 Behavior of propagation constant, α , with increasing mode number .	25
3 Efficiency as function of increasing mode number for both fast and slow modes	28
4 Behavior of $Z[J_1(Z)/J_0(Z)]$ as function of Z showing periodicity of values of Z that satisfy equation (92)	30
5 Propagation constant, α , as function of increasing mode number ...	33
6 Efficiency as function of mode number for both fast and slow modes	39

TABLES

1 Analysis of Ribbon Beam, Approximate Roots	23
2 Analysis of Ribbon Beam, Exact Roots	24
3 Analysis of Ribbon Beam, Efficiency	28

TABLES (Cont'd)

	<u>Page</u>
4 Analysis of Cylindrical Beam, Approximate Roots	32
5 Analysis of Cylindrical Beam, Exact Roots	33
6 Analysis of Cylindrical Beam, Efficiency	38

1. INTRODUCTION

In an earlier examination of the Cerenkov radiation of charged particles passing over a dielectric plate,* it was noted that, under certain conditions, a beam of these particles could support a number of intrinsic electromagnetic modes. This was a surprising result, as we had not before encountered a discussion of these modes, and a search of the available literature turned up only one study of these modes, with a brief analysis, for slab geometries only, of the results.¹ In view of the relevance of this topic and our findings to the expanding field of near-millimeter waves, we decided to continue our analysis.

This report discusses the derivation of the interaction between the electromagnetic field and the electron beam. Although this derivation may be found in many books containing sections on Cerenkov radiation or monographs on travelling-wave devices,^{2,3} the derivation appears here to familiarize the reader with our particular notation and assumptions. This derivation generates the wave equations satisfied by components of the electromagnetic fields within a suitably restricted electron beam. The theory applies to the case of a ribbon type of electron beam in free space. It is demonstrated that the form of the wave equation for this situation suggests a superficial resemblance between the propagation constants of an electron beam and those of a dielectric of identical geometry. By selecting some realistic parameters (such as current density and beam size), we find a few modes of ribbon beam.

¹Istvan Palocz, *A Leaky Wave Approach to Cerenkov and Smith-Purcell Radiation*, Ph.D. Dissertation, Polytechnic Institute of Brooklyn, University Microfilms, Inc., Ann Arbor, MI, #62-5658 (1962).

²M. Chodorow and C. Susskind, *Fundamentals of Microwave Electronics*, McGraw-Hill Book Co., New York (1964), 141-177.

³R. G. E. Hutter, *Beam and Wave Electronics in Microwave Tubes*, D. Van Nostrand Co., New York (1960), 182-233.

*Clyde A. Morrison and Richard P. Leavitt, *Cerenkov Radiation from an Electron Beam Passing over a Dielectric Slab Backed by a Metal Surface*, Harry Diamond Laboratories (draft).

This same procedure is then used to find the modes of a cylindrical beam in free space. Because no available literature deals with this case, we examine these modes in considerable detail and discuss the amount of energy coupled out of these modes.

2. ELECTRON BEAM WAVE EQUATIONS

These are Maxwell's equations listed in the form used in this report:

$$\nabla \times \vec{H} = -ik\vec{E} + (4\pi/c)\vec{J}_t \quad , \quad (1)$$

$$\nabla \times \vec{E} = ik\vec{H} \quad , \quad (2)$$

$$\nabla \cdot \vec{H} = 0 \quad , \quad (3)$$

$$\nabla \cdot \vec{E} = 4\pi\rho_t \quad , \quad (4)$$

where \vec{H} and \vec{E} vary as $e^{-i\omega t}$ and $k = \omega/c$. In equations (1) to (4), \vec{H} and \vec{E} are the magnetic and electric fields, \vec{J}_t is the current density, and ρ_t is the charge density. Unrationalized cgs units are used throughout this report. We make the following linearizing approximations:

$$\rho_t = \rho_0 + \rho \quad , \quad (5)$$

$$\vec{V}_t = v_0 \hat{e}_z + \vec{V} \quad , \quad (6)$$

$$\vec{J}_t = J_0 \hat{e}_z + \vec{J} \quad , \quad (7)$$

where ρ_0 , v_0 , and J_0 are constant in time and space and ρ , \vec{V} , and \vec{J} vary as $e^{-i\omega t}$. We assume that ρ , \vec{V} , and \vec{J} are small in comparison with ρ_0 , v_0 , and J_0 . Also,

$$\vec{J}_t = \rho_t \vec{V}_t \quad . \quad (8)$$

The Lorentz force equation is used here in the form

$$\frac{d}{dt} (\gamma \vec{V}_t) = - \frac{e}{m} \left(\vec{E} + \frac{\vec{V}_t}{c} \times \vec{H} \right) \quad . \quad (9)$$

Here,

$$\gamma = 1/(1 - v_t^2/c^2)^{1/2}$$

and

$$\frac{d}{dt} \equiv \frac{\partial}{\partial t} + \vec{V}_t \cdot \nabla \quad .$$

From equations (1) and (4) comes the conservation condition

$$\dot{\rho}_t + \nabla \cdot \vec{J}_t = 0 \quad . \quad (10)$$

Inserting equations (5), (6), and (7) into equation (8) and keeping only first order terms, we obtain

$$\vec{J}_0 = \rho_0 v_0 \hat{e}_z \quad , \quad (11)$$

$$\vec{J} = \rho \hat{e}_z v_0 + \rho_0 \vec{v} \quad . \quad (12)$$

Note that all variables in equation (11) are constant with respect to time and position.

The next step is to search for travelling-wave solutions of the fundamental equations. We assume that, for all functions of z ,

$$F(x, y, z) = F(x, y) e^{iaz} \quad .$$

Using equation (9) and the above assumptions, the following expressions are found:

$$v_x = - \frac{ie(E_x - \beta H_y)}{m\gamma^3(\omega - \alpha v)} \quad , \quad (13)$$

$$v_y = - \frac{ie(E_y + \beta H_x)}{m\gamma^3(\omega - \alpha v)} \quad , \quad (14)$$

$$v_z = - \frac{ieE_z}{m\gamma^3(\omega - \alpha v)} \quad , \quad (15)$$

where $\beta = v/c$.

By substituting equations (13), (14), and (15) into equation (12), we get these results for the components of \vec{J} :

$$J_x = \frac{i\omega^2(E_x - \beta H_y)}{4\pi\gamma^3(\omega - \alpha V)} \quad , \quad (16)$$

$$J_y = \frac{i\omega^2(E_y + \beta H_x)}{4\pi\gamma^3(\omega - \alpha V)} \quad , \quad (17)$$

$$J_z = \frac{i\omega^2 E_z}{4\pi\gamma^3(\omega - \alpha V)} \quad , \quad (18)$$

where $\frac{\omega^2}{p} = -4\pi n_0 e^2/m$. To derive equation (18), it is necessary to use equations (16) and (17) in equations (10) and (4). Doing so gives also

$$\rho = \frac{i\beta\omega^2 E_z}{4\pi\gamma c(\omega - \alpha V)} \quad . \quad (19)$$

We can now get the wave equation for our beam by taking the curl of equation (1) and using equations (2), (16), (17), and (18):

$$\nabla_{\vec{t}}^2 \vec{H} + \left(k^2 - \alpha^2 - \frac{\omega^2}{c^2\gamma^3} \right) \vec{H} = 0 \quad , \quad (20)$$

and similarly for \vec{E} ,

$$\nabla_{\vec{t}}^2 \vec{E} + \left(k^2 - \alpha^2 - \frac{\omega^2}{c^2\gamma^3} \right) \vec{E} = 0 \quad , \quad (21)$$

where

$$\nabla_t^2 \equiv \frac{\partial^2}{\partial x^2} + \frac{\partial^2}{\partial y^2} .$$

Except for a change in propagation, these equations are the same as one would find for an ordinary medium. There are two sets of solutions corresponding to transverse magnetic (TM) and transverse electric (TE) modes.

3. RESTRICTED BEAM

Consider now an electron beam restricted such that $V_x = 0$, $V_y = 0$, and as before (eq 15) we have

$$V_z = \frac{-ieE_z}{m\gamma^3(\omega - \alpha V)} . \quad (22)$$

The assumption that $V_x = V_y = 0$ is physically realizable with the application of a strong magnetic field in the z-direction.

Also, $J_x = 0$, $J_y = 0$, and from continuity ($\omega\rho = \alpha J_z$) we obtain

$$J_z = \frac{i\omega^2\omega E_z}{4\pi\gamma^3(\omega - \alpha V)^2} \quad (23)$$

and

$$\rho = \frac{i\alpha\omega^2 E_z}{4\pi\gamma^3(\omega - \alpha V)^2} \quad (24)$$

The restriction on the beam has a considerable effect, as can be noted by comparing equation (23) with equation (18) and equation (24) with equation (19). Using equations (1) to (4), we can find the wave equation

$$\nabla(\nabla \cdot \vec{E}) - \nabla^2 \vec{E} = k^2 \vec{E} + ik \frac{4\pi}{c} \vec{J} \quad (25)$$

which can be written in component form as

$$\frac{\partial}{\partial x} (4\pi\rho) - \nabla^2 E_x = k^2 E_x \quad (26)$$

$$\frac{\partial}{\partial y} (4\pi\rho) - \nabla^2 E_y = k^2 E_y \quad (27)$$

$$\frac{\partial}{\partial z} (4\pi\rho) - \nabla^2 E_z = k^2 E_z + ik \frac{4\pi}{c} J_z \quad (28)$$

Substituting equations (23) and (24) into equation (28) yields

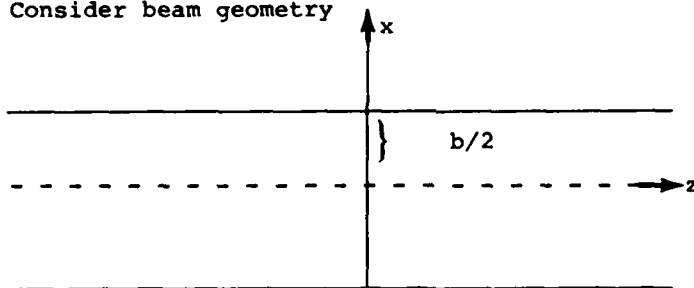
$$\nabla^2 E_z + k^2 E_z = \frac{k}{c} \left[\frac{\omega^2 \omega E_z}{\gamma^3(\omega - \alpha V)^2} \right] - \frac{\alpha^2 \omega^2 E_z}{\gamma^3(\omega - \alpha V)^2} \quad (29)$$

$$\nabla_z^2 E_z + (k^2 - \alpha^2) \left[1 - \frac{k_p^2}{\gamma^3 (k - \alpha\beta)^2} \right] E_z = 0 \quad , \quad (30)$$

where $k_p^2 = \omega^2/c^2$. This equation is frequently encountered in discussions of travelling-wave devices.² The factor $k_p^2/\gamma^2(k - \alpha\beta)^2$ gives rise to solutions for α near $\alpha\beta = k$, in which the phase velocity of the wave is nearly equal to the velocity of the electrons in the beam. The beam must be restricted in order to generate these additional solutions. No such behavior is possible from the wave equations for the unrestricted beam given in equations (20) and (21).

3.1 Ribbon Beam

Consider beam geometry



where the y-axis is perpendicular to the paper. Assume the beam to be infinite in the y- and z-directions and $\partial/\partial y = 0$. Then, in component form, Maxwell's equations become

$$-\alpha E_y = ikH_x \quad , \quad -i\alpha H_y = -ikE_x \quad , \quad (31a,b)$$

$$i\alpha E_x = ikH_y + \frac{\partial E_z}{\partial x} \quad , \quad i\alpha H_x = -ikE_y \quad , \quad (32a,b)$$

²M. Chodorow and C. Susskind, *Fundamentals of Microwave Electronics*, McGraw-Hill Book Co., New York (1964), 141-177.

$$\frac{\partial}{\partial x} E_y = -ikH_z \quad , \quad \frac{\partial}{\partial x} H_y = ikE_z + \frac{4\pi}{c} J_z \quad , \quad (33a,b)$$

$$\frac{\partial}{\partial x} E_x + i\alpha E_z = 4\pi\rho \quad , \quad \frac{\partial}{\partial x} H_x = i\alpha H_z \quad . \quad (34a,b)$$

Further, considering TM modes only, $H_z = 0$, which from equations (31) to (34) immediately gives $E_y = 0$ and $H_x = 0$. From equations (31b) and (32a),

$$H_y = \frac{ik}{k^2 - \alpha^2} \frac{\partial}{\partial x} E_z \quad (35)$$

for all values of x .

Inside the beam, equation (30) becomes

$$\frac{\partial^2}{\partial x^2} E_z + (k^2 - \alpha^2) \left[1 - \frac{k_p^2}{\gamma^3 (k - \alpha\beta)^2} \right] E_z = 0 \quad , \quad (36)$$

and outside the beam $k_p = 0$ so that

$$\frac{\partial^2}{\partial x^2} E_z + (k^2 - \alpha^2) E_z = 0 \quad . \quad (37)$$

The symmetry of this geometry allows one to choose either even or odd solutions to these equations; thus, we can restrict ourselves to $x > 0$. Looking at the even solutions, then, we can write

$$E_z = A \cos(k_1 x) e^{i\alpha z} \quad , \quad 0 \leq x \leq b/2 \quad , \quad (38)$$

and

$$E_z = B e^{ik_2 x} e^{iaz} \quad , \quad b/2 \leq x \quad , \quad (39)$$

where

$$k_1^2 = (k^2 - \alpha^2) \left[1 - \frac{k_p^2}{\gamma^3 (k - \alpha\beta)^2} \right] \quad (40)$$

and

$$k_2^2 = (k^2 - \alpha^2) \quad , \quad (41)$$

and A and B are arbitrary constants.

Also, from equation (35) we can write

$$H_y = \frac{ik}{k^2 - \alpha^2} \left[-k_1 A \sin(k_1 x) e^{iaz} \right] \quad , \quad 0 \leq x \leq b/2 \quad , \quad (42)$$

$$H_y = \frac{ik}{k^2 - \alpha^2} \left(ik_2 B e^{ik_2 x} e^{iaz} \right) \quad , \quad b/2 \leq x \quad . \quad (43)$$

Continuity of E_z and H_y at $x = b/2$ yields

$$A \cos\left(\frac{k_1 b}{2}\right) = B e^{ik_2 b/2} \quad (44)$$

and

$$-k_1 A \sin\left(\frac{k_1 b}{2}\right) = ik_2 B e^{ik_2 b/2} \quad (45)$$

Dividing equation (45) by equation (44) gives the following transcendental equation:

$$-k_1 \tan\left(\frac{k_1 b}{2}\right) = ik_2 \quad (46)$$

This expression has no solutions if both k_1 and k_2 are real. Assume that k_1 is real and $k_2 = ik_2'$, where k_2' is real. Thus, k_2' must be positive if $e^{ik_2 x}$ is to decay and produce bound modes outside the beam. Also, from equation (41),

$$k_2'^2 = \alpha^2 - k^2 \quad (47)$$

so

$$k_1^2 = -k_2^2 \left[1 - \frac{k_2^2}{\gamma^3 (k - \alpha\beta)^2} \right] \quad (48)$$

Now equation (48) satisfies the assumption that k_1 is real only when

$$\frac{k_2^2}{\gamma^3 (k - \alpha\beta)^2} > 1 \quad (49)$$

One can rewrite equation (46) as

$$\tan \left\{ \frac{b}{2} (\alpha^2 - k^2)^{1/2} \left[\frac{k_p^2}{\gamma^3 (k - \alpha\beta)^2} - 1 \right]^{1/2} \right\}$$

(50)

$$= \left[\frac{k_p^2}{\gamma^3 (k - \alpha\beta)^2} - 1 \right]^{1/2} .$$

For a given set of parameters such as electron density, velocity, and beam width, there are successive values of α that satisfy equation (50). Each of these values corresponds to a mode whose phase velocity is ω/α . Further analysis of these modes, including the calculation of these modes for a certain set of conditions, follows in section 4.1.

3.2 Cylindrical Beam

The discussion in section 3.1 (up to eq 30) applies to any restricted beam where $V_x = V_y = 0$. Thus, the examination of the cylindrical beam begins with equation (30). This time, in order to impose cylindrical symmetry on the problem, we will let $\partial/\partial\theta = 0$. In this case, the component forms of equations (1) and (2) become, recalling that $F(r, \theta, z) = F(r, \theta)e^{i\alpha z}$,

$$ikH_r = -i\alpha E_\theta \quad , \quad -ikE_r = i\alpha H_\theta \quad , \quad (51a,b)$$

$$ikH_{\theta} = i\alpha E_r - \frac{\partial}{\partial r} E_z, \quad -ikE_{\theta} = i\alpha H_r, \quad (52a,b)$$

$$ikH_z = \frac{1}{r} \frac{\partial}{\partial r} (rE_{\theta}), \quad -ikE_z + \frac{4\pi}{c} J_z = \frac{1}{r} \frac{\partial}{\partial r} (kH_{\theta}) \quad (53a,b)$$

Here again, to get TM modes, H_z is set to 0. Solving for E_r in equation (51b) and substituting the solution into equation (52a), we have

$$H_{\theta} = \frac{ik}{k^2 - \alpha^2} \frac{\partial}{\partial r} E_z, \quad (54)$$

and equation (30) can be written as

$$\left(\frac{\partial^2}{\partial r^2} + \frac{1}{r} \frac{\partial}{\partial r} + k_1^2 \right) E_z = 0, \quad r \leq a, \quad (55)$$

$$\left(\frac{\partial^2}{\partial r^2} + \frac{1}{r} \frac{\partial}{\partial r} - k_2'^2 \right) E_z = 0, \quad r \geq a, \quad (56)$$

where k_1^2 and $k_2'^2$ are defined as before and a is the radius of the beam. These are Bessel's equations and have solutions,

$$E_z = \begin{cases} AJ_0(k_1 r) & , \quad r \leq a \\ BK_0(k_2' r) & , \quad r \geq a \end{cases} \quad (57)$$

where A and B are constants.

Using equations (51b) and (54) and the Bessel recursion formula,⁴ we find for $r \leq a$

$$\frac{d}{dx} [x^{-n} J_n(x)] = -x^{-n} J_{n+1}(x) ,$$

$$E_z = AJ_0(k_1 r) , \quad (58)$$

$$E_r = -\frac{iak_1}{k_2^2} AJ_1(k_1 r) , \quad (59)$$

$$H_\theta = -\frac{ikk_1}{k_2^2} AJ_1(k_1 r) , \quad (60)$$

and we find for $r \geq a$

$$E_z = BK_0(k_2' r) , \quad (61)$$

$$E_r = -\frac{iak_2'}{k_2^2} BK_1(k_2' r) , \quad (62)$$

$$H_\theta = -\frac{ikk_2'}{k_2^2} BK_1(k_2' r) . \quad (63)$$

Both sets of solutions must agree at $r = a$ so that

⁴M. Abramowitz and I. A. Stegun, *Handbook of Mathematical Functions*, National Bureau of Standards (November 1970), 355-434.

$$AJ_0(k_1 a) = BK_0(k_2' a) \quad (64)$$

and H_0 must be continuous, giving

$$Ak_1 J_1(k_1 a) = Bk_2' K_1(k_2' a) \quad (65)$$

Dividing equation (65) by equation (64) yields

$$\frac{k_1 J_1(k_1 a)}{k_2' J_0(k_1 a)} = \frac{K_1(k_2' a)}{K_0(k_2' a)} \quad (66)$$

Once more, the values of α that satisfy this relation represent modes that can propagate down the beam. Section 4 contains analyses of equations (50) and (66), including the determination of some modes for both cases.

4. ANALYSIS OF BEAMS

4.1 Analysis of Ribbon Beam

For a ribbon beam of thickness b , the modes that can propagate are determined by solving equation (50). So in terms of k_1 and k_2' ,

$$\tan\left(\frac{k_1 t}{2}\right) = \frac{k_2'}{k_1} \quad (67)$$

Let us begin by defining g and η such that

$$g = \frac{k^2}{\gamma^3 k^2} \quad , \quad \eta = 1 - \frac{a}{k} \beta \quad . \quad (68a,b)$$

Equation (50) becomes

$$\tan \left\{ \frac{kb}{2\beta} [(1 - \eta)^2 - \beta^2]^{1/2} \left(\frac{g^2}{\eta^2} - 1 \right)^{1/2} \right\} = \left(\frac{g^2}{\eta^2} - 1 \right)^{-1/2} \quad . \quad (69)$$

To justify some of the following approximations, it is appropriate to define what we consider realistic values for the parameters of equation (69). The current state of electron beam devices makes relativistic beams with currents of several amperes obtainable, depending on the size of the beam. The values used here are designed to describe a system with a relativistic beam, $\beta = 0.7$ typically, and a current of about 200 mA for a cylindrical beam of 0.5-cm radius. This current yields an electron density, n_0 , of about 7.5×10^7 electrons/cm³. These same numbers are used for the ribbon beam. Because of the interest of producing power sources with operating frequencies between 200 and 300 GHz, we consider an output wavelength of 1 mm. In summary, the calculations are carried out with the following values:

$$\lambda = 0.1 \text{ cm} \quad ,$$

$$b, a = 0.5 \text{ cm} \quad ,$$

$$n_0 = 7.5 \times 10^7 / \text{cm}^3 ,$$

$$\beta = 0.7 ,$$

which correspond to 198 mA for the cylindrical beam or 252 mA/cm² for the sheet beam (recall that we did not specify a boundary in the y-direction).

To continue with the analysis, to get real arguments for equation (69), η must be between $+g$ and $-g$. For the values of k_p , k , and β , g is fairly small (about 1.5×10^{-4}), so we first let

$$z = \left(\frac{g^2}{\eta^2} - 1 \right)^{1/2} \quad (70)$$

and then make the approximation $\eta \approx 0$ in the expression

$$[(1 - \eta)^2 - \beta^2]^{1/2} \sim 1/\gamma .$$

Now equation (69) can be written as

$$z \tan \left(\frac{kb}{2\beta\gamma} z \right) = 1 . \quad (71)$$

Finally, we further simplify the argument of tan by letting

$$z = \frac{kb}{2\beta\gamma} z \quad (72)$$

so that

$$Z \tan Z = \frac{kb}{2\beta\gamma} \quad (73)$$

The roots, Z_m , of equation (73) are not difficult to find. A brief glance at the function $Z \tan Z$ shows that there must be values of Z in every π interval that satisfy equation (73). Figure 1 illustrates this result for the case where g , b , and β have the values chosen earlier. Only the positive portion of $Z \tan Z$ has been plotted. Table 1 contains the calculated values of Z corresponding to the first 11 modes.

The third column, $Z \tan Z \sim kb/2\beta\gamma$, gives some indication of the accuracy of the roots.

Combining equations (70) and (72) gives

$$\eta = \pm \left[\frac{g^2}{1 + \left(\frac{2\beta\gamma}{kb}\right)^2 Z^2} \right]^{1/2} \quad (74)$$

Thus, for every value of Z there are two values of η to be considered in the exact case, that is, when η is no longer approximated as zero in $[(1 - \eta)^2 - \beta^2]^{1/2}$. In this way, two values of α are generated corresponding to "fast" and "slow" solutions of equation (50). Table 2 contains the fast and slow propagation constants for the first 11 modes.

The fast solutions, corresponding to smaller α 's, are found by taking the positive case in equation (74). Slow solutions are generated by using the negative case.

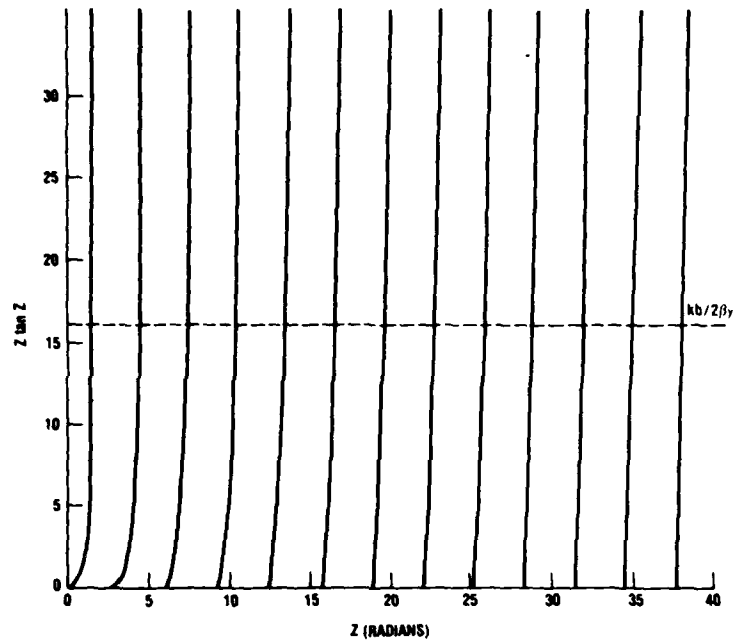


Figure 1. Behavior of $Z \tan Z$ as function of Z demonstrating periodicity of values of Z that satisfy equation (73): $\lambda = 0.1$ cm, $b = 0.5$ cm, and $\beta = 0.7$.

TABLE 1. ANALYSIS OF RIBBON BEAM,
 APPROXIMATE ROOTS: $\lambda = 0.1$ cm,
 $b = 0.5$ cm, $n_o = 7.5 \times 10^7/\text{cm}^3$,
 AND $\beta = 0.7$

Mode number, m	Z	$Z \tan Z - kb/2\beta\lambda$
0	1.47878	1.144×10^{-5}
1	4.44199	9.5367×10^{-6}
2	7.42034	6.485×10^{-5}
3	10.4191	0.0
4	13.4393	9.5367×10^{-6}
5	16.4794	-2.0981×10^{-5}
6	19.5365	2.4795×10^{-5}
7	22.6078	5.722×10^{-6}
8	25.0905	3.6239×10^{-5}
9	28.7824	3.2424×10^{-5}
10	31.8817	2.6703×10^{-5}

TABLE 2. ANALYSIS OF RIBBON BEAM,
 EXACT ROOTS: $\lambda = 0.1$ cm, $b = 0.5$ cm,
 $n_0 = 7.5 \times 10^7/\text{cm}^3$, AND $\beta = 0.7$

Mode number, m	α fast	α slow
0	89.7459	89.7739
1	89.7464	89.7734
2	89.7472	89.7726
3	89.7481	89.7716
4	89.7491	89.7706
5	89.7501	89.7697
6	89.7510	89.7688
7	89.7518	89.7680
8	89.7525	89.7673
9	89.7531	89.7667
10	89.7536	89.7662

One can see from figure 2 that, as the mode number increases, the difference between a fast and a slow decreases. In fact, a fast and a slow converge to the value of α that would yield a phase velocity equal to the particle velocity of the beam; that is, $\alpha = k/\beta$.

It is possible to investigate the ratio of energy flowing outside the beam to that flowing inside for various modes by integrating the average Poynting vector over a cross section of the beam. Thus, we want to evaluate

$$\int_S \vec{S}_{av} \cdot d\vec{a} = \frac{1}{2} \int_S \text{Re}(\vec{E} \times \vec{H}^*) \cdot d\vec{a} \quad (75)$$

Since we are interested in energy flowing in the z-direction and $H_x = H_z = E_y = 0$,

$$W = \frac{1}{2} \int_S \text{Re}(E_x H_y^*) dx dy \quad (76)$$

$$H_y^* = \frac{-ik}{k^2 - \alpha^2} [-k_1 A \sin(k_1 x) e^{-i\alpha z}] \quad (77)$$

$$E_x = \frac{i\alpha}{k^2 - \alpha^2} [-k_1 A \sin(k_1 x) e^{i\alpha z}] \quad (78)$$

thus, for $-b/2 < x < b/2$,

$$W_I = \int_0^1 \int_0^{b/2} \frac{\alpha k}{(k^2 - \alpha^2)^2} k_1^2 A^2 \sin^2(k_1 x) dx dy, \quad (79)$$

where W_I is the energy per centimeter length in the y-direction. Integrating equation (79), we obtain

$$W_I = \frac{\alpha k k_1^2 A^2}{(k^2 - \alpha^2)^2} \left(b - \frac{1}{k} \sin k_1 b \right). \quad (80)$$

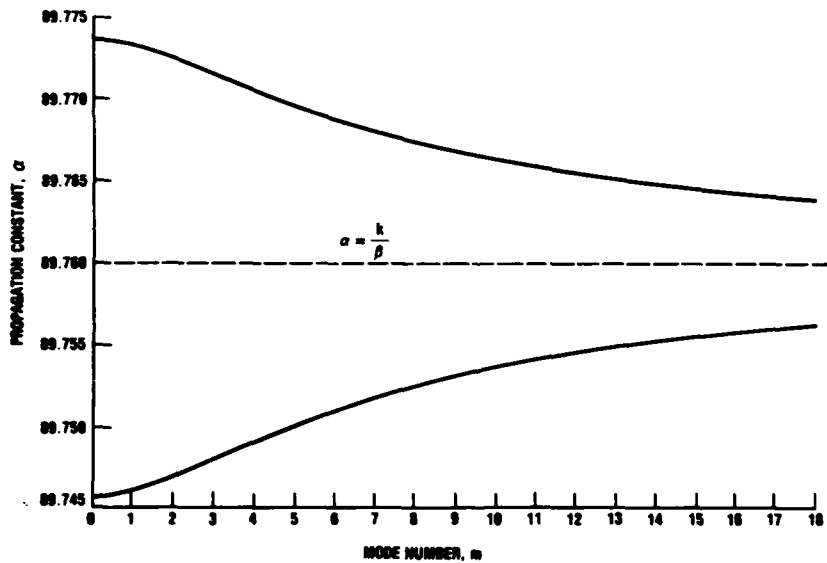


Figure 2. Behavior of propagation constant, α , with increasing mode number; values above $\alpha = k/\beta$ are propagation constants for fast modes and those below correspond to slow modes: $\lambda = 0.1$ cm, $b = 0.5$ cm, $n_0 = 7.5 \times 10^7/\text{cm}^3$, and $\beta = 0.7$.

Outside the beam,

$$H_y^* = \frac{k}{k^2 - \alpha^2} (ik_2' B e^{-k_2' x} e^{-i\alpha z}) \quad , \quad (81)$$

$$E_x = \frac{-\alpha}{k^2 - \alpha^2} (ik_2' B e^{-k_2' x} e^{i\alpha z}) \quad ; \quad (82)$$

thus, the energy flowing outside the beam, W_0 , is

$$W_0 = \int_0^1 \int_{b/2}^{\infty} \frac{\alpha k}{(k^2 - \alpha^2)^2} k_2'^2 B^2 e^{-2k_2' x} dx dy \quad (83)$$

$$= \frac{\alpha k k_2' B^2}{2(k^2 - \alpha^2)^2} e^{-k_2' b} \quad . \quad (84)$$

From equation (45), we have

$$B = \frac{k_1 A}{k_2'} \sin\left(\frac{k_1 b}{2}\right) e^{k_2' b/2} \quad , \quad (85)$$

so equation (84) becomes

$$W_0 = \frac{\alpha k_1^2 k A^2}{2k_2' (k^2 - \alpha^2)^2} \sin^2\left(\frac{k_1 b}{2}\right) \quad . \quad (86)$$

In equations (80) and (86), A is determined by the manner in which the beam is perturbed from its ideal steady-state condition. Such perturbations are nearly inevitable, but very difficult to predict. We can nevertheless consider the ratio of these energies independent of A. Thus, after cancellation of the common constants,

$$\frac{W_0}{W_0 + W_I} = \frac{\frac{1}{2k_2'} \sin^2 \left(\frac{k_1 b}{2} \right)}{\frac{1}{2k_2'} \sin^2 \left(\frac{k_1 b}{2} \right) + b - \frac{1}{k_1} \sin k_1 b} \quad (87)$$

$$= \frac{\sin^2 \left(\frac{k_1 b}{2} \right)}{\sin^2 \left(\frac{k_1 b}{2} \right) + 2k_2' b - 2 \frac{k_2'}{k_1} \sin k_1 b} \quad (88)$$

Hereafter, $W_0/(W_0 + W_I)$ is referred to as Q. Table 3 contains values for Q for the first 10 modes.

Figure 3 compares the energy ratios for these modes. For the first mode, at least, the slow waves are more efficient, coupling a larger percentage of the energy outside of the beam. Even with the first mode, however, Q is less than 1.7 percent. For both fast and slow waves, the efficiency is monotonically decreasing with increasing mode number.

TABLE 3. ANALYSIS OF RIBBON BEAM, EFFICIENCY:
 $\lambda = 0.1$ cm, $b = 0.5$ cm, $n_0 = 7.5 \times 10^7/\text{cm}^3$,
 AND $\beta = 0.7$

Mode number, m	Q fast	Q slow
0	1.57364×10^{-2}	1.69584×10^{-2}
1	1.51604×10^{-2}	1.50324×10^{-2}
2	1.32180×10^{-2}	1.32568×10^{-2}
3	1.12045×10^{-2}	1.17251×10^{-2}
4	9.31548×10^{-3}	9.15241×10^{-3}
5	7.69732×10^{-3}	7.80541×10^{-3}
6	6.61363×10^{-3}	6.10717×10^{-3}
7	5.55854×10^{-3}	5.67797×10^{-3}
8	4.62158×10^{-3}	4.74057×10^{-3}
9	3.46832×10^{-3}	3.58016×10^{-3}

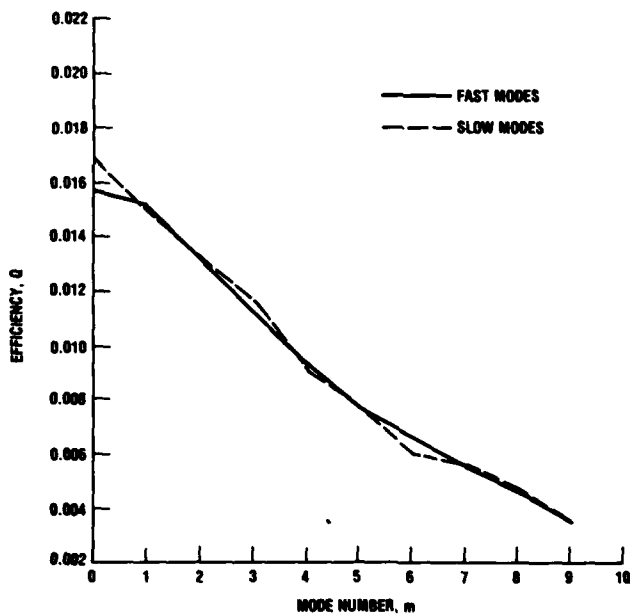


Figure 3. Efficiency as function of increasing mode number for both fast and slow modes: $\lambda = 0.1$ cm, $b = 0.5$ cm, $n_0 = 7.5 \times 10^7/\text{cm}^3$, and $\beta = 0.7$.

4.2 Analysis of Cylindrical Beam

For a cylindrical beam of radius a , we derived the relations

$$\frac{k_1 J_1(k_1 a)}{k_2' J_0(k_1 a)} = \frac{K_1(k_2' a)}{K_0(k_2' a)} \quad (89)$$

where k_1 and k_2' are defined as before.

If we again define g and η as in equations (68a) and (68b), then

$$\left(\frac{g^2}{\eta^2} - 1\right)^{1/2} \frac{J_1 \left\{ \frac{ka}{\beta} [(1-\eta)^2 - \beta^2]^{1/2} \left(\frac{g^2}{\eta^2} - 1\right)^{1/2} \right\}}{J_0 \left\{ \frac{ka}{\beta} [(1-\eta)^2 - \beta^2]^{1/2} \left(\frac{g^2}{\eta^2} - 1\right)^{1/2} \right\}} = \frac{K_1 \left\{ \frac{ka}{\beta} [(1-\eta)^2 - \beta^2]^{1/2} \right\}}{K_0 \left\{ \frac{ka}{\beta} [(1-\eta)^2 - \beta^2]^{1/2} \right\}} \quad (90)$$

As with the ribbon beam, we let $z = (g^2/\eta^2 - 1)^{1/2}$ and make the approximation $\eta \sim 0$ in $[(1-\eta)^2 - \beta^2]^{1/2}$. Then equation (90) becomes

$$z \frac{J_1\left(\frac{ka}{\beta\gamma} z\right)}{J_0\left(\frac{ka}{\beta\gamma} z\right)} = \frac{K_1\left(\frac{ka}{\beta\gamma}\right)}{K_0\left(\frac{ka}{\beta\gamma}\right)} \quad (91)$$

From the previous procedure and equation (72),

$$z = \frac{ka}{\beta\gamma} z$$

so that we have

$$Z \frac{J_1(Z)}{J_0(Z)} = \frac{ka}{\beta\gamma} \frac{K_1\left(\frac{ka}{\beta\gamma}\right)}{K_0\left(\frac{ka}{\beta\gamma}\right)} \quad (92)$$

The evaluation of this expression is not too difficult, especially when one recognizes that the right-hand side of equation (92) is constant. Now, $J_0(Z)$ and $J_1(Z)$ have zeros occurring with the same frequency in Z . Thus, we would expect $J_1(Z)/J_0(Z)$ to reach any value between $-\infty$ and $+\infty$ once between each zero of, say, $J_0(Z)$. This range is illustrated in figure 4.

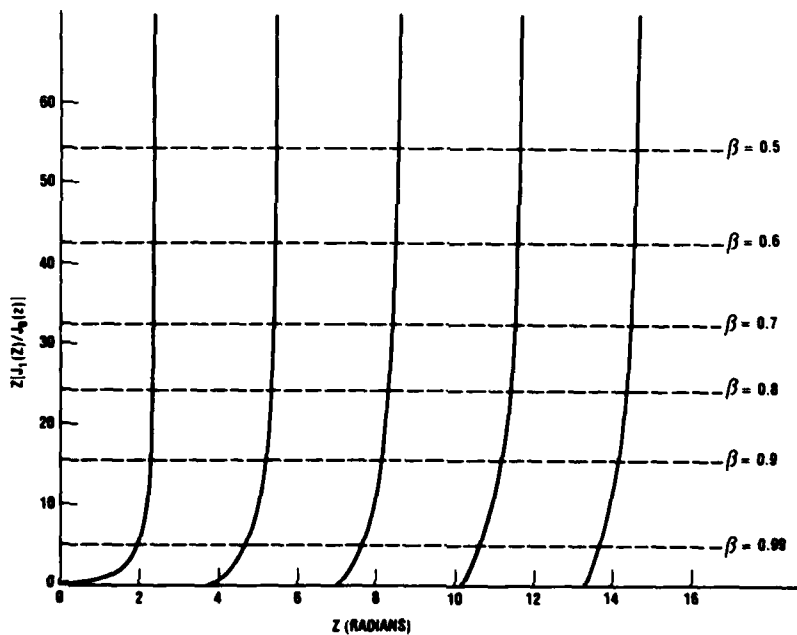


Figure 4. Behavior of $Z[J_1(Z)/J_0(Z)]$ as function of Z showing periodicity of values of Z that satisfy equation (92): $\lambda = 0.1$ cm, $a = 0.5$ cm, and different values of β .

By Hankel's asymptotic expansion⁴ for large Z ,

$$J_\nu(Z) = 4\pi Z P(\nu, Z) \cos x - Q(\nu, Z) \sin x \quad ,$$

$$x = Z - \left(\frac{1}{2}\nu + \frac{1}{4}\right)\pi \quad ,$$

where

$$P(\nu, Z) \sim 1 - \frac{(4\nu^2 - 1)(4\nu^2 - 9)}{2!(8Z)^2} \\ + \frac{(4\nu^2 - 1)(4\nu^2 - 9)(4\nu^2 - 25)(4\nu^2 - 49)}{2!(8Z)^4} - \dots$$

and

$$Q(\nu, Z) \sim \frac{(4\nu^2 - 1)}{8Z} - \frac{(4\nu^2 - 1)(4\nu^2 - 9)(4\nu^2 - 25)}{3!(8Z)^2} + \dots \quad ,$$

we can write, keeping only the first order terms,

$$\frac{J_1(Z)}{J_0(Z)} \approx \tan\left(Z - \frac{\pi}{4}\right) \quad , \quad Z \text{ large} \quad , \quad (93)$$

which explains the tangent-like behavior in figure 3.

⁴M. Abramowitz and I. A. Stegun, *Handbook of Mathematical Functions*, National Bureau of Standards (November 1970), 355-434.

In the actual calculation of equation (92), a short power-series routine was used for small values of Z . Machine limitations reduced accuracy for $Z > 10$, so we resorted to Hankel's expansion for larger values. It was found, however, that the second order terms were necessary to achieve the desired accuracy for Z near 10. Table 4 contains some results for realistic parameters.

TABLE 4. ANALYSIS OF CYLINDRICAL BEAM, APPROXIMATE
ROOTS: $\lambda = 0.1$ cm, $a = 0.5$ cm, $\beta = 0.7$, AND
 $X = ka/\beta\lambda$

Mode number, m	Z_m	$ZJ_1(Z)/J_0(Z)$	$XK_1(X)/K_0(X)$
0	2.33219	32.5468	32.5468
1	5.35454	32.5470	32.5468
2	8.39744	32.5460	32.5468
3	11.4489	32.5469	32.5468
4	14.5062	32.5476	32.5468
5	17.5699	32.5468	32.5468
6	20.6397	32.5472	32.5468
7	23.7156	32.5468	32.5468
8	26.7972	32.5468	32.5468
9	29.8843	32.5469	32.5468
10	32.9763	32.5474	32.5468
11	36.0728	32.5467	32.5468

As with the ribbon beam, we used equation (74) and plugged back into the exact expression, equation (90). Table 5 lists the fast and slow roots. These results are plotted in figure 5. Once again, the fast and slow propagation constants are converging to the phase velocity of a wave travelling at the particle velocity of the beam. This time, however, they are approaching this value at a slower rate than with the ribbon beam.

TABLE 5. ANALYSIS OF CYLINDRICAL BEAM, EXACT ROOTS:
 $\lambda = 0.1$ cm, $a = 0.5$ cm, $n_0 = 7.5 \times 10^7/\text{cm}^3$, AND
 $\beta = 0.7$

Mode number, m	Z (approx)	α fast	α slow
0	2.33219	89.74579622	89.77378403
1	5.35454	89.74595104	89.77362938
2	8.39744	89.74621742	89.77336329
3	11.4489	89.74657698	89.77300407
4	14.5062	89.74700762	89.77257377
5	17.5699	89.74748676	89.77209494
6	20.6397	89.74799375	89.77158820
7	23.7156	89.74851130	89.77107083
8	26.7972	89.74902600	89.77055625
9	29.8843	89.74952809	89.77005422

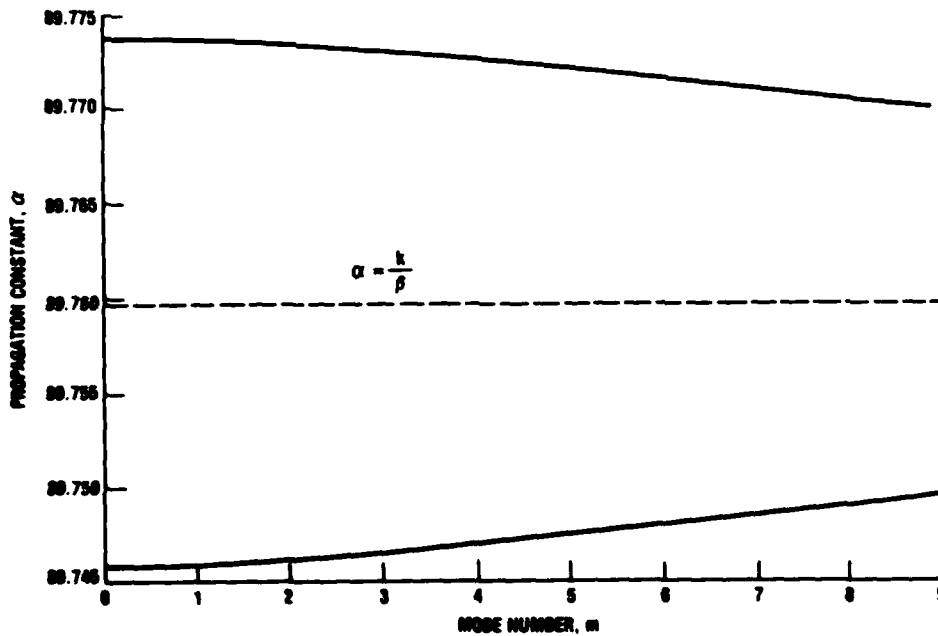


Figure 5. Propagation constant, α , as function of increasing mode number; values of α above and below $\alpha = k/\beta$ correspond to fast and slow modes, respectively: $\lambda = 0.1$ cm, $a = 0.5$ cm, $n_0 = 7.5 \times 10^7/\text{cm}^3$, and $\beta = 0.7$.

The calculation using the average Poynting vector is a little more complicated for this geometry, but it is still relatively straightforward. As before, the expression to evaluate is equation (75),

$$\int_S \vec{S}_{av} \cdot d\vec{a} = \frac{1}{2} \int_S \text{Re}(\vec{E} \times \vec{H}^*) \cdot d\vec{a} \quad ,$$

and again we are concerned with energy travelling in the z-direction and with TM modes, so

$$W = \frac{1}{2} \int_S \text{Re}(E_r H_\theta^*) r \, dr \, d\theta \quad . \quad (94)$$

For $r < a$,

$$H_\theta^* = \frac{ikk_1}{k_2^2} AJ_1(k_1 r) \quad , \quad (95)$$

$$E_r = \frac{-iak_1}{k_2^2} AJ_1(k_1 r) \quad , \quad (96)$$

which, when substituted into equation (94), gives

$$W_I = \frac{akk_1^2}{2k_2^4} A^2 \int_0^{2\pi} \int_0^a J_1^2(k_1 r) r \, dr \, d\theta \quad . \quad (97)$$

Now,

$$\int_0^x t J_1^2(ut) dt = \frac{x^2}{2} [J_1^2(ux) - J_0(ux)J_2(ux)] \quad , \quad (98)$$

which holds also for k_1^2 in the integrand,⁵ so

$$W_I = \frac{\pi \alpha k k_1^2}{(k^2 - \alpha^2)^2} A^2 \frac{a^2}{2} [J_1^2(k_1 a) - J_0(k_1 a)J_2(k_1 a)] \quad , \quad (99)$$

or since

$$J_2(k_1 a) = \frac{2}{k_1 a} J_1(k_1 a) - J_0(k_1 a) \quad ,$$

$$W_I = \frac{\pi \alpha k k_1^2}{(k^2 - \alpha^2)^2} A^2 \frac{a^2}{2} [J_0^2(k_1 a) + J_1^2(k_1 a) \quad (100)$$

$$- \frac{2}{k_1 a} J_0(k_1 a)J_1(k_1 a)] \quad .$$

⁵E. D. Rainville, *Special Functions*, Macmillan Publishing Co., New York (1960), 108-119.

Similarly, for $r > a$,

$$H_{\theta}^* = \frac{ikk_2'}{k^2 - \alpha^2} BK_1(k_2'r) \quad , \quad (101)$$

$$E_r = - \frac{iak_2'^2}{k^2 - \alpha^2} BK_1(k_2'r) \quad , \quad (102)$$

which yields

$$W_0 = \frac{\alpha k k_2'^2}{2(k^2 - \alpha^2)^2} B^2 \int_0^{2\pi} \int_a^{\infty} K_1^2(k_2'r) r \, dr \, d\theta \quad , \quad (103)$$

and from equation (97),

$$W_0 = - \frac{\pi \alpha k k_2'^2}{(k^2 - \alpha^2)^2} B \frac{a^2}{2} \left[K_1^2(k_2'a) - K_0(k_2'a) K_2(k_2'a) \right] \quad . \quad (104)$$

Here,

$$K_2(k_2'a) = \frac{2}{k_2'a} K_1(k_2'a) + K_0(k_2'a) \quad ,$$

so

$$w_0 = \frac{\pi \alpha k k_2'^2}{(k^2 - \alpha^2)^2} B^2 \frac{a^2}{2} \left[\kappa_0^2(k_2'a) - \kappa_1^2(k_2'a) \right]$$

(105)

$$+ \frac{2}{k_2'a} \kappa_0(k_2'a) \kappa_1(k_2'a) \quad .$$

We can use equation (64) to solve for B:

$$B = \frac{AJ_0(k_1a)}{\kappa_0(k_2'a)} \quad .$$

(106)

Utilizing equation (106),

$$w_0 = \frac{\pi \alpha k k_2'^2}{(k^2 - \alpha^2)^2} A^2 \frac{a^2}{2} \frac{J_0^2(k_1a)}{\kappa_0(k_2'a)}$$

(107)

$$\times \left[\kappa_0^2(k_2'a) - \kappa_1^2(k_2'a) + \frac{2}{k_2'a} \kappa_0(k_2'a) \kappa_1(k_2'a) \right]$$

$$= \frac{\pi \alpha k k_2'^2}{(k^2 - \alpha^2)^2} A^2 \frac{a^2}{2} J_0^2(k_1a)$$

(108)

$$\times \left[1 - \frac{\kappa_1^2(k_2'a)}{\kappa_0^2(k_2'a)} + \frac{2}{k_2'a} \frac{\kappa_1(k_2'a)}{\kappa_0(k_2'a)} \right] \quad .$$

As with the sheet beam, these expressions for the energy are not useful without some way to specify A, but the ratio of $W_O/(W_O + W_I)$ is independent of A. We have, then,

$$\frac{W_O}{W_O + W_I} = \frac{k_2'^2 J_0^2 \left(1 - \frac{K_1^2}{K_0^2} + \frac{2}{k_2' a} \frac{K_1}{K_0} \right)}{k_2'^2 J_0 \left(1 - \frac{K_1^2}{K_0^2} + \frac{2}{k_2' a} \frac{K_1}{K_0} \right) + k_1^2 \left(J_0^2 + J_1^2 - \frac{2}{k_2' a} J_0 J_1 \right)}, \quad (109)$$

where the argument of J_0 and J_1 is $k_1 a$ and that of K_0 and K_1 is $k_2' a$.

Table 6 contains some calculated values for $W_O/(W_O + W_I)$ (which is called Q). These values are plotted in figure 6. These efficiencies are roughly twice as large as those of the ribbon beam and have a smoother behavior as the mode number increases. Consistently for any mode number, slow waves couple out more energy.

TABLE 6. ANALYSIS OF CYLINDRICAL BEAM, EFFICIENCY:
 $\lambda = 0.1$ cm, $a = 0.5$ cm, $n_o = 7.5 \times 10^7/\text{cm}^3$,
 AND $\beta = 0.7$

Mode number, m	Q fast	Q slow
0	3.20058×10^{-2}	3.32486×10^{-2}
1	3.12990×10^{-2}	3.25074×10^{-2}
2	3.01073×10^{-2}	3.12456×10^{-2}
3	2.85307×10^{-2}	2.95827×10^{-2}
4	2.67009×10^{-2}	2.76532×10^{-2}
5	2.47362×10^{-2}	2.55864×10^{-2}
6	2.27388×10^{-2}	2.34890×10^{-2}
7	2.07866×10^{-2}	2.14423×10^{-2}
8	1.89319×10^{-2}	1.95021×10^{-2}
9	1.72068×10^{-2}	1.77009×10^{-2}

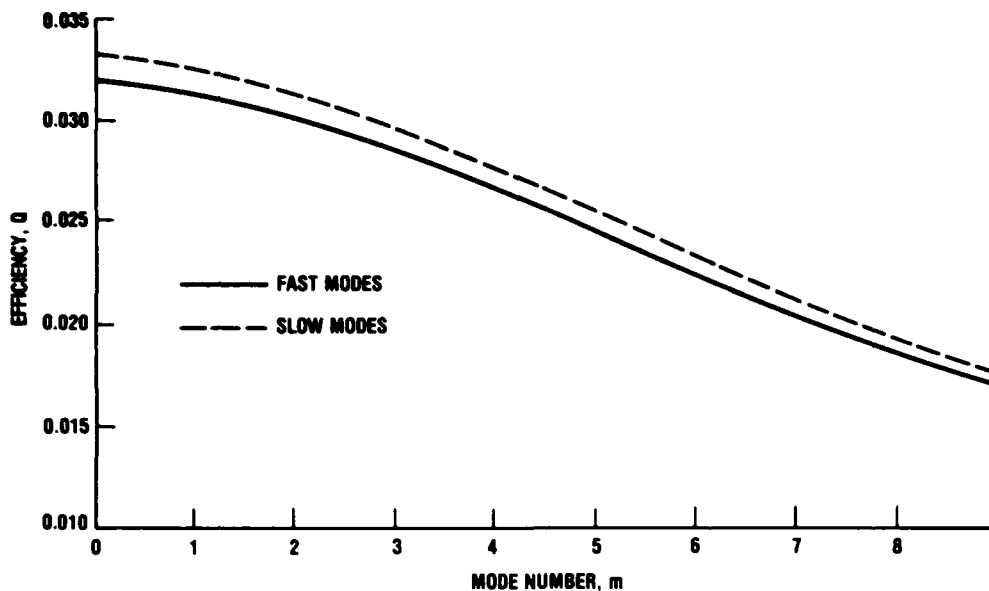


Figure 6. Efficiency as function of mode number for both fast and slow modes: $\lambda = 0.1$ cm, $a = 0.5$ cm, $n_0 = 7.5 \times 10^7/\text{cm}^3$, and $\beta = 0.7$.

5. CONCLUSIONS

Except in the ideal case of a perfectly unperturbed electron beam, bound electromagnetic modes will be propagating down a beam of charged particles in free space. The behavior of these modes is quite similar for both the beam geometries considered. In fact, for both types, the dispersion relations produce similar values for the propagation constant. This similarity is not surprising since the dispersion relation for the cylindrical beam can be characterized by a tangent function for larger arguments and the ribbon beam dispersion relation is in fact a tangent function.

It was interesting to examine the percentage of energy flowing outside the beam because if an attempt to use these modes were made, one

would almost certainly try to couple to them outside the beam. For our parameters, the maximum efficiency for a single mode was little more than 3 percent. Although the numbers were very similar, the slow modes couple out slightly more of the total electromagnetic energy.

A more difficult problem is to be able to predict and characterize perturbations on the beam in the laboratory. In addition to increasing our understanding of the beam's behavior, it might enable us to excite the beam for some desired result.

The problems considered here should not be taken as a result, but as a step toward the solution of more complicated problems. Of immediate technological interest is the inducement of Cerenkov radiation in the millimeter wave range. The regions outside the beam considered here could be occupied by dielectric or partially filled with dielectric. The ribbon beam case considered here could be applied to the dielectric configuration considered previously.* The calculation of the fraction of the total energy propagated outside the electron beam could be repeated for the Cerenkov radiation induced in the dielectric slab. Such calculations could be used to optimize parameters of the system for the production of Cerenkov radiation of a particular, predetermined frequency.

ACKNOWLEDGEMENT

The authors are indebted to Richard P. Leavitt of the Harry Diamond Laboratories for his constructive criticism of all phases of the work presented here.

*Clyde A. Morrison and Richard P. Leavitt, *Cerenkov Radiation from an Electron Beam Passing over a Dielectric Slab Backed by a Metal Surface*, Harry Diamond Laboratories (draft).

LITERATURE CITED

- (1) Istvan Palocz, A Leaky Wave Approach to Cerenkov and Smith-Purcell Radiation, Ph.D. Dissertation, Polytechnic Institute of Brooklyn, University Microfilms, Inc., Ann Arbor, MI, #62-5658 (1962).
- (2) M. Chodorow and C. Susskind, Fundamentals of Microwave Electronics, McGraw-Hill Book Co., New York (1964), 141-177.
- (3) R. G. E. Hutter, Beam and Wave Electronics in Microwave Tubes, D. Van Nostrand Co., New York (1960), 182-233.
- (4) M. Abramowitz and I. A. Stegun, Handbook of Mathematical Functions, National Bureau of Standards (November 1970), 355-434.
- (5) E. D. Rainville, Special Functions, Macmillan Publishing Co., New York (1960), 108-119.

DISTRIBUTION

ADMINISTRATOR
DEFENSE TECHNICAL INFORMATION CENTER
ATTN DTIC-DDA (12 COPIES)
CAMERON STATION
ALEXANDRIA, VA 22314

COMMANDER
US ARMY RES, DEV & STANDARDIZATION
GROUP (EUR)
ATTN CHIEF, ELECTRONICS BRANCH
ATTN CHIEF, MATHEMATICS & PHYSICS
BRANCH
ATTN CHIEF, MATERIALS BRANCH
BOX 65
FPO NEW YORK 09510

COMMANDER
US ARMY MISSILE & MUNITIONS CENTER
& SCHOOL
ATTN ATSK-CTD-F
REDSTONE ARSENAL, AL 35809

DIRECTOR
US ARMY MATERIEL SYSTEMS ANALYSIS
ACTIVITY
ATTN DRXSJ-MP
ABERDEEN PROVING GROUND, MD 21005

DIRECTOR
ELECTRONICS TECHNOLOGY & DEVICES
LABORATORY
ATTN DELET-DD
ATTN DELET-D, TECHNICAL DIRECTOR
ATTN DELET-B, N. J. WILSON
ATTN DELET-M, DR. H. HIESLMAIR
ATTN TECHNICAL LIBRARY
ATTN CHARLES DESANTIS
FT MONMOUTH, NJ 07703

HQ USAF/SAMI
WASHINGTON, DC 20330

TELEDYNE BROWN ENGINEERING
CUMMINGS RESEARCH PARK
ATTN DR. MELVIN L. PRICE, MS-44
HUNTSVILLE, AL 35807

ENGINEERING SOCIETIES LIBRARY
ATTN ACQUISITIONS DEPARTMENT
345 EAST 47TH STREET
NEW YORK, NY 10017

COMMANDER
US ARMY ATMOSPHERIC SCIENCES LABORATORY
ATTN TECHNICAL LIBRARY
WHITE SANDS MISSILE RANGE, NM 88002

COMMANDER/DIRECTOR
COMBAT SURVEILLANCE & TARGET ACQUISITION
LABORATORY
ATTN TECHNICAL LIBRARY
FT MONMOUTH, NJ 07703

DIRECTOR
ELECTRONIC WARFARE LABORATORY
ATTN TECHNICAL LIBRARY
FT MONMOUTH, NJ 07703

DIRECTOR
NIGHT VISION & ELECTRO-OPTICS LABORATORY
ATTN TECHNICAL LIBRARY
ATTN DELNV-L, DR. R. BUSER
FT BELVOIR, VA 22060

DIRECTOR
US ARMY SIGNALS WARFARE LABORATORY
VINT HILL FARMS STATION
ATTN TECHNICAL LIBRARY
WARRENTON, VA 22186

UNDER SECRETARY OF DEFENSE RE & ENG
ATTN DEP UNDER SECRETARY RE & ADVANCED
TECHNOLOGY
WASHINGTON, DC 20301

OFFICE OF ASSISTANT SECRETARY OF THE ARMY
RE, DEV & ACQ
ATTN PRINCIPAL DEPUTY ASSISTANT SECRETARY
(RAD)
ATTN DIR OF ARMY RES
DAMA-ARZ-A, DR. M. E. LASSER
DEPARTMENT OF THE ARMY
WASHINGTON, DC 20310

COMMANDER
US ARMY MATERIEL DEV & READINESS COMMAND
ATTN DRCLDC, J. BENDER
5001 EISENHOWER AVE
ALEXANDRIA, VA 22333

COMMANDER
US ARMY RESEARCH OFFICE (DURHAM)
ATTN DR. R. LONTZ
ATTN DR. J. SUTTLE
ATTN DR. W. FLOOD
PO BOX 12211
RESEARCH TRIANGLE PARK, NC 27709

COMMANDING OFFICER
US ARMY FOREIGN SCIENCE & TECHNOLOGY
CENTER
FEDERAL OFFICE BLDG
ATTN TECHNICAL LIBRARY
220 7TH STREET, NE
CHARLOTTSVILLE, VA 22901

DISTRIBUTION (Cont'd)

COMMANDER
US ARMY MISSILE COMMAND
ATTN TECHNICAL LIBRARY
ATTN CHIEF, RESEARCH DIRECTORATE
REDSTONE ARSENAL, AL 35809

COMMANDER
US ARMY ARMAMENT RES & DEV COMMAND
ATTN TECHNICAL LIBRARY
DOVER, NJ 07801

COMMANDER
US ARMY COMMUNICATIONS & ELECTRONICS
MATERIEL READINESS COMMAND
ATTN TECHNICAL LIBRARY
FT MONMOUTH, NJ 07703

CHIEF OF NAVAL RESEARCH
DEPT OF THE NAVY
ATTN TECHNICAL LIBRARY
ARLINGTON, VA 22217

SUPERINTENDENT
NAVAL POSTGRADUATE SCHOOL
ATTN LIBRARY, CODE 2124
MONTEREY, CA 93940

DIRECTOR
NAVAL RESEARCH LABORATORY
ATTN 2600, TECHNICAL INFO DIV
ATTN DR. V. L. GRANATSTEIN
ATTN DR. PHILIP SPRANGLE
WASHINGTON, DC 20375

COMMANDER
NAVAL SURFACE WEAPONS CENTER
ATTN DX-21, LIBRARY DIV
DAHLGREN, VA 22448

COMMANDER
NAVAL SURFACE WEAPONS CENTER
ATTN E-40, TECHNICAL LIBRARY
WHITE OAK, MD 20910

COMMANDER
NAVAL WEAPONS CENTER
ATTN TECHNICAL LIBRARY
CHINA LAKE, CA 93555

COMMANDER
HQ AIR FORCE SYSTEMS COMMAND
ANDREWS AFB
ATTN TECHNICAL LIBRARY
WASHINGTON, DC 20334

SECRETARY
DEPARTMENT OF ENERGY
G-234
ATTN DR. M. JOHNSON
ATTN DR. M. MURPHY
ATTN DR. J. WILLIS
WASHINGTON, DC 20545

COLUMBIA UNIVERSITY
DEPARTMENT OF ELECTRICAL ENGINEERING
ATTN DR. S. P. SCHLESINGER
NEW YORK, NY 10027

STANFORD UNIVERSITY
SLAC
ATTN DR. JEAN LEBACQZ
STANFORD, CA 94305

DARTMOUTH COLLEGE
PHYSICS DEPARTMENT
ATTN DR. JOHN WALSH
HANOVER, NH 03755

US ARMY ELECTRONICS RESEARCH &
DEVELOPMENT COMMAND
ATTN TECHNICAL DIRECTOR, DRDEL-CT

HARRY DIAMOND LABORATORIES
ATTN CO/TD/TSO/DIVISION DIRECTORS
ATTN RECORD COPY, 81200
ATTN HDL LIBRARY, 81100 (2 COPIES)
ATTN HDL LIBRARY, 81100 (WOODBIDGE)
ATTN TECHNICAL REPORTS BRANCH, 81300
ATTN CHAIRMAN, EDITORIAL COMMITTEE
ATTN LEGAL OFFICE, 97000
ATTN CHIEF, 00210
ATTN CHIEF, 11000
ATTN CHIEF, 13000
ATTN CHIEF, 15000
ATTN CHIEF, 21300
ATTN CHIEF, 22000
ATTN CHIEF, 95000
ATTN H. BRANDT, 22300
ATTN O. MEYER, 22800
ATTN Z. G. SZTANKAY, 13300
ATTN N. KARAYIANIS, 13200
ATTN J. MCGARRITY, 22300
ATTN J. NEMARICH, 13300
ATTN J. SILVERSTEIN, 13300
ATTN R. MORRISON, 13500
ATTN J. SOLN, 22300
ATTN R. CURNUTT, 13300
ATTN R. LEAVITT, 13200
ATTN G. D. DOCKERY, 13300 (10 COPIES)
ATTN C. MORRISON, 13200 (10 COPIES)

FILMED
5-8